JOURNAL OF PLANKTON RESEARCH | VOLUME 34 | NUMBER 9 | PAGES 739–748 | 2012

Pelagic community responses to a deep-water front in the California Current Ecosystem: overview of the A-Front Study

MICHAEL R. LANDRY[1]*, MARK D. OHMAN[1]*, RALF GOERICKE[1], MICHAEL R. STUKEL[2], KATHERINE A. BARBEAU[1], RANDELLE BUNDY[1] AND MATI KAHRU[1]

[1]SCRIPPS INSTITUTION OF OCEANOGRAPHY, UNIVERSITY OF CALIFORNIA SAN DIEGO, LA JOLLA, CA, USA AND [2]HORN POINT LABORATORY, UNIVERSITY OF MARYLAND CENTER FOR ENVIRONMENTAL SCIENCE, CAMBRIDGE, MD, USA

*CORRESPONDING AUTHORS: mlandry@ucsd.edu (M.R.L.); mohman@ucsd.edu (M.D.O.)

Received November 4, 2011; accepted in principle March 11, 2012; accepted for publication March 18, 2012

Corresponding editor: Roger Harris

In October 2008, we investigated pelagic community composition and biomass, from bacteria to fish, across a sharp frontal gradient overlying deep waters south of Point Conception, California. This north–south gradient, which we called A-Front, was formed by the eastward flow of the California Current and separated cooler mesotrophic waters of coastal upwelling origin to the north, from warm oligotrophic waters of likely mixed subarctic–subtropical origin to the south. Plankton biomass and phytoplankton growth rates were two to three times greater on the northern side, and primary production rates were elevated 5-fold to the north. Compared with either of the adjacent waters, the frontal interface was strongly enriched and uniquely defined by a subsurface bloom of large diatoms, elevated concentrations of suspension-feeding zooplankton, high bioacoustical estimates of pelagic fish and enhanced bacterial production and phytoplankton biomass and photosynthetic potential. Such habitats, though small in areal extent, may contribute disproportionately and importantly to regional productivity, nutrient cycling, carbon fluxes and trophic ecology. As a general introduction to the A-Front study, we provide an overview of its design and implementation, a brief summary of major findings and a discussion of potential mechanisms of plankton enrichment at the front.

KEYWORDS: fronts; phytoplankton; zooplankton; iron; nutrients; California Current

INTRODUCTION

The California Current (CC) system is a region of complex hydrography that extends for more than 2000 km along the west coast of North America, from close to the US–Canadian border on its northern end to south of the US–Mexican border to the south, and seaward typically for 300–500 km. The major currents include the southward-flowing CC, which brings cool and relatively fresh waters from the subarctic Pacific down the coast, a persistent but temporally variable undercurrent that brings warmer saltier waters of equatorial origin northward over the continental slope, and

doi:10.1093/plankt/fbs025, available online at www.plankt.oxfordjournals.org. Advance Access publication April 24, 2012

© The Author 2012. Published by Oxford University Press. All rights reserved. For permissions, please email: journals.permissions@oup.com

Downloaded from http://plankt.oxfordjournals.org/ at University of California, San Diego on October 19, 2012

the northward flowing Inshore Countercurrent (Lynn and Simpson, 1987), which is referred to as the Davidson Current when it outcrops the surface of the inner shelf during the winter (Hickey, 1998). Offshore, the CC is bounded by warm salty waters of the central North Pacific. Inshore, equatorward winds during summer drive strong coastal upwelling close to shore and weaker wind-curl upwelling over most of the region, bringing cool saline waters with high nutrients to the surface (Hill *et al.*, 1998). Such areas of enrichment can extend far to sea, sometimes associated with the meandering flows around eddies and coastal promontories (Marchesiello *et al.*, 2003; Centurioni *et al.*, 2008), but typically bounded on their outer edge by the core inshore edge of the CC. The interaction of the current core with the mesoscale eddy field results in a complex zone of variable width that largely contains the richer habitats along the coast (Strub *et al.*, 1991). Within and between the on- and offshore habitats, there exists a richness of interacting fronts and small-scale dynamical features and a mosaic of plankton assemblages with varying contents and compositions. Fronts and eddies are especially prevalent within a 500–700 km wide band along the coast (Kahru *et al.*, 2012).

Fronts, eddies and other mesoscale features are known to be areas of elevated plankton biomass and activity in many regions (Franks, 1992; Fiala *et al.*, 1994; Pitcher *et al.*, 1998; Basterretxea and Aristegui, 2000; Jacquet *et al.*, 2002; Brown *et al.*, 2008). They thus can represent enriched habitats that contribute disproportionately to regional productivity, nutrient cycling, carbon fluxes and trophic ecology. In the southern CC ecosystem, for example, Loggerwell and coworkers have suggested that recruitment success of Pacific sardine may be related to climate-related variability in mesoscale eddies (Loggerwell *et al.*, 2001). Recent studies have also pointed to the potential importance of subduction at fronts as an explanation for the massive imbalance of new versus export production that arises when only contemporaneous processes in homogeneous water parcels are considered (e.g. Stukel *et al.*, 2011). Despite their implied importance, however, the biological characteristics and ecological roles of fronts in the CC are poorly resolved. In two notable studies conducted to date, Hood *et al.* (Hood *et al.*, 1991) found that the larger size fraction of chlorophyll was enriched on the shoreward side of a front off central California, while Haury *et al.* concluded that a prominent front off Ensenada, Mexico, marked only a transition in water masses, without a local impact on plankton biomass, composition or productivity (Haury *et al.*, 1993; Venrick, 2000). Neither of these studies was robust in the scope of the measurements undertaken or the resolution of sampling across the feature of interest. It remains therefore to be determined how mesoscale features and fronts in the CC contribute to understanding of regional ecological processes.

As a first step to systematic studies to answer that question, we investigated the distributional patterns of plankton assemblages, from bacteria to fish, across a sharp frontal transition (which we designate the A-Front) sampled in October 2008 on a cruise of the California Current Ecosystem, Long-Term Ecological Research (CCE-LTER) program. Detailed results for various aspects of the study are presented in seven papers in this issue. As a general introduction to the A-Front study, here we provide an overview of its design and implementation, some results that compare characteristics of the water masses sampled on both sides of the front, a brief summary of major findings and relationships in the detailed papers that follow, and a common discussion that relates to potential mechanisms of plankton enrichment at the front.

THE STUDY SITE

The A-Front study was conducted from 22 to 28 October 2008 on CCE-LTER process cruise P0810 on the *R/V Melville*. The study was given its name ("A") because we envisioned it to be the first in a series of broader investigations of system responses to the different types of fronts and mesoscale features in the southern CCE region. For this particular investigation, we looked mainly for a site with sharp persistent surface features that could be rapidly sampled (therefore semi-synoptically) with short station spacing during the dark period of a single night. Prior to the cruise, October was determined to be historically the month of lowest percentage cloud cover and highest frequency of satellite ocean color data in the southern CCE region. We in fact had excellent daily and composite image coverage of both sea surface temperature (SST) and ocean color to monitor frontal features in the area throughout the month, except for a strong storm in early October, which broadly enhanced Chl *a* concentrations in the coastal waters around Point Conception. We selected for the A-Front study a well-defined east–west-oriented feature located south of Point Conception and well offshore of the California Channel Islands (Fig. 1). The location is in the area where CC, forced by local winds and the sharp bend in the coastline at Point Conception, takes an abrupt turn toward the east, before redirecting southward parallel to the coast (Pares-Sierra and O'Brien, 1989). The specific study site

Downloaded from http://plankt.oxfordjournals.org/ at University of California, San Diego on October 19, 2012

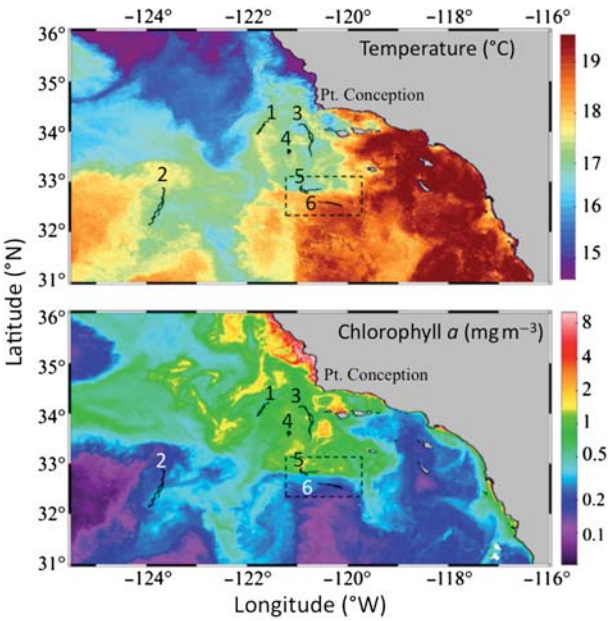

Fig. 1. Satellite images of SST (°C) and near-surface chlorophyll *a* (mg Chl *a* m^{-3}) in the southern CC ecosystem. SST is merged from MODIS-Aqua and MODIS-Terra data for 22–25 October 2008. Chl *a* is merged from MERIS, MODIS-Aqua, MODIS-Terra and SeaWiFS data for 22–25 October. Dashed box is the A-Front study region shown in Fig. 2. Drifter tracks of experimental Cycles 1–6 conducted during CCE Process cruise P0810 are shown in solid lines; cycle numbers are placed on the side indicating initial deployment positions.

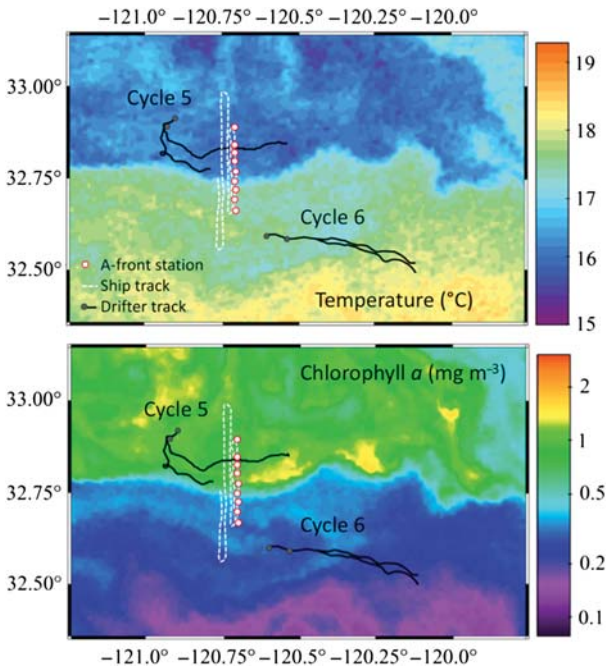

Fig. 2. Expanded view of the A-Front study region (from Fig. 1) showing ship tracks during underway crossings of the front (white dashed lines), locations of CTD/net tow sampling stations for the transect study (red circles), and the 2-day drifter paths for experimental process Cycles 5 and 6 (dots show start positions; sediment trap array moves to the front during Cycle 5).

is 350 km due west of San Diego, California (32.7°N), and overlies water of 3700-m depth.

Previous investigations of fronts in the southern CCE region have also highlighted an east–west-oriented feature, which has been called the Ensenada Front (Niiler *et al.*, 1989; Haury *et al.*, 1993; Chereskin and Niiler, 1994; Venrick, 2000). Chereskin and Niiler (Chereskin and Niiler, 1994) used that name broadly to describe all of the flow features that begin with the eastward sweep of the CC south of Point Conception and end in the branched terminus of an inverted "T" hundreds of kilometers to the south. In contrast, Venrick (Venrick, 2000) more narrowly depicted the Ensenada Front as only the terminal branched area, where relatively weak gradients mark the southern boundary of surface chlorophyll and temperature signatures of the CC where it collides with warmer waters of subtropical origin. Here, the A-Front is a very sharp gradient separating coastal upwelling water from mixed CC and subtropical waters. While it resided in the northern part of the broad Ensenada Front domain of currents and mesoscale features described by Chereskin and Niiler, it is distinguished in location, hydrography and ecological characteristics from the specific frontal feature that was studied earlier (Venrick, 2000).

STUDY DESIGN AND IMPLEMENTATION

The A-Front study was designed with three major elements: underway survey sampling with multiple crossings of the front, a rapid transect of stations sampled across the front and process studies in the adjacent water masses that interact at the front (Fig. 2). The study began with 2 days, 22–24 October, of experimental process studies on the north side of the front (Cycle 5 in Fig. 2). Following that, five underway front crossings, denoted by dashed white lines in Fig. 2, were completed between 1000 and 2100 on 24 October, ending south of the front. These were immediately followed by rapid station sampling during the night (21:30 to 05:00) of 24–25 October, ending north of the front. Additional process studies were then conducted from 26 to 28 October on the south side of the front (Cycle 6, Fig. 2). In describing these elements below, we begin with the transect crossings, which are central to most of the papers in this theme section. The process experiments are then briefly described, mainly as context for comparing ecological conditions in the waters north and south of the front.

Downloaded from http://plankt.oxfordjournals.org/ at University of California, San Diego on October 19, 2012

Underway sampling

Four initial underway crossings of the front were done rapidly, at 20 km h^{-1} ship speed, to establish the coherence of the cross-frontal features in our local working area (Ohman *et al.*, 2012). The underway transect lines were initially ~50-km long to probe significantly into the adjacent water masses, but they were shortened to 25 km in the final two crossings, which were done at reduced speed (10 km h^{-1}) for finer spatial resolution. In addition to routine measurements of surface hydrography (ship's thermosalinograph) and subsurface currents (Acoustical Doppler Current Profiling), the underway surveys employed three major instrument systems for various measures of hydrography, phytoplankton, zooplankton and micronekton. A free-falling Moving Vessel Profiler (MVP, ODIM Brooke Ocean) was equipped with a CTD, fluorometer and Laser Optical Plankton Counter (LOPC) (Herman *et al.*, 2004) to measure temperature, salinity, density, *in vivo* Chl *a* and size and optical characteristics of large particles (aggregates and zooplankton) in depth profiles to 200 m (Ohman *et al.*, 2012). An Advanced Laser Fluorometer (ALF, Chekalyuk and Hafez, 2008) plumbed to the ship's uncontaminated seawater line (bow inlet ~4.5 m) measured near-surface Raman-normalized fluorescence signals associated with Chl *a*, phycobiliproteins (*Synechococcus* and eukaryotic cryptophytes), chromophoric dissolved organic matter and photo-physiological status (variable fluorescence, F_v/F_m) of the autotrophic community (Chekalyuk *et al.*, 2012). A pole-mounted multi-beam echosounder (SIMRAD EK-60 equipped with 38, 70, 120 and 200 kHz transducers) was used to assess the distributions of migratory and non-migratory krill and fish down to 750-m depth (Lara Lopez *et al.*, 2012). The final underway survey run was conducted after darkness (18:50–21:00) on 24 October to avoid non-photochemical quenching of photosynthetic pigments and to capture the nocturnal vertical distributions of migratory animals. The relatively slow speed of that run was optimal for the acoustical system and provided 1.1-km spacing of MVP drops and ~16-m resolution for the ALF surface measurements.

Transect sampling

Directly following the final underway transect, we resampled the same transect in the opposite direction by deploying a CTD-rosette-video profiling package and taking a vertical net tow for zooplankton at each of nine stations (circles in Fig. 2, between 21:30 and 05:00 local time). For the latter, we used a vertically retrieved bongo net (0.71-m diameter, 202-μm mesh) with weighted cod ends (cf. Ohman and Wilkinson, 1989). The net was lowered to 100-m depth and recovered at 30 m min^{-1}. Composition and size structure were determined by ZooScan digital scanning and image analysis of the formaldehyde-preserved animals (Gorsky *et al.*, 2010; Ohman *et al.*, 2012).

CTD casts at the transect stations were taken to 300 m. On the down casts, we used a digital camera system with columnar illumination (Underwater Video Profiler5; Picheral *et al.*, 2010; Ohman *et al.*, 2012) attached to the bottom of the rosette frame to image undisturbed 1-L volumes of seawater at 6 Hz. On the up casts, seven to eight rosette bottles (10-L Niskin) were tripped "on-the-fly" at depths that defined the major features observed in Chl *a* fluorescence on the down cast (i.e. surface, middle and base of the mixed layer, shoulders and peaks of the subsurface Chl *a* maximum layer and 80 and 100 m at all stations). On board, the bottles were subsampled for dissolved nutrients, total organic carbon, total nitrogen, particulate organic carbon and nitrogen, total dissolved carbohydrates, transparent particles, phytoplankton Chl *a* and accessory pigments (fluorometry, high performance liquid chromatography and ALF), and abundance and biomass of bacteria, phytoplankton and heterotrophic protists (flow cytometry and epifluorescence microscopy). At selected stations and depths, water samples were also taken to assess viral abundance, production rates of heterotrophic bacteria (^{3}H-leucine; Samo *et al.*, 2012) and photosynthesis versus light energy relationships for the phytoplankton assemblage (Wang *et al.*, 2008).

Process studies

In contrast to the sampling at fixed transect stations, the process studies were conducted as Lagrangian-based experiments following satellite-tracked drogued drifters. On one drift array, VERTEX tube-style sediment traps (Knauer *et al.*, 1979) were deployed at the base of the euphotic zone (60 m) and at 100 m at the beginning and recovered at the end of each 2-day experiment. The second drift array was used for rate assessments of primary production, phytoplankton growth and microzooplankton grazing. Drift arrays employed a holey sock drogue centered at a depth of 15 m, following the WOCE drifter design of Niiler *et al.* (Niiler *et al.*, 1995), and utilized Globalstar communications. The water column was sampled in the vicinity of the drift array in the early morning of each day, using the CTD-rosette to collect water for the standard suite of hydrographic, chemical and biological measurements (as above) and

Downloaded from http://plankt.oxfordjournals.org/ at University of California, San Diego on October 19, 2012

to set up ^{14}C-primary production experiments and two-treatment dilution experiments for each of eight depths spanning the euphotic zone (as described in Landry *et al.*, 2009; Stukel *et al.*, 2011). These experiments were incubated under *in situ* conditions of temperature and light for 24 h in net bags attached to a line under the surface float, and they were replaced by a new set of experiments on the following morning. Using the drifter as a moving frame of reference, we conducted additional sampling throughout the day, including mid-day measurements of bio-optical variables (Wang *et al.*, 2008), mid-day and mid-night depth-stratified net tows for mesozooplankton with a 1-m^2 MOCNESS (Ohman, personal communication), day and nighttime sampling of mesopelagic organisms with 5-m^2 Matsuda-Oozeki-Hu trawl (Lara Lopez *et al.*, 2012), water-column and pump samples to assess carbon export by the ^{234}Thorium method (Stukel *et al.*, 2011), and trace-metal clean sampling with GO-Flo bottles and synthetic hydroline to assess the concentration of total dissolved iron using a sulfite reduction method with chemiluminescence detection (King and Barbeau, 2007, 2011).

CHARACTERISTICS OF THE A-FRONT AND ADJACENT WATERS

The A-Front was located in a region of complex hydrography at the boundary of cooler coastal waters to the north and warmer waters to the south (Fig. 1). Drifter experiments conducted earlier during the P0810 cruise (Fig. 1; notably Cycle 3, 15–18 October; http://cce.lternet.edu/data/cruises/cce-p0810/data/) suggest that waters originating from the upwelling region around Point Conception had a strong southerly flow toward the A-Front area. The relative richness of the northern side of the front also derives from its being in an area of generally positive wind stress curl (Rykaczewski and Checkley, 2008). Far offshore of the A-Front site, the CC, marked by the flow of low salinity core water, was southwestward (Cycle 2, 9–14 October; http://cce.lternet.edu/data/cruises/cce-p0810/data/)). In the A-Front study area, however, flows both to the north and to the south of the front were strongly toward the east (0.2–0.3 m s^{-1}).

Results from process experiments conducted to the north (Cycle 5) and south (Cycle 6) of the A-Front illustrate the contrasting states of the adjacent waters (Table I). For most euphotic zone-integrated estimates of standing stocks, values north of the front were about two to three times higher than those to the south.

Table I: Comparison of measured characteristics of waters sampled north and south of A-Front during experimental Cycles 5 and 6

Variable	North: Cycle 5	South: Cycle 6
Mixed-layer depth (m)	23 ± 8	29 ± 8
Nitracline depth (m), 1 μM nitrate	2.1 ± 0.7	37 ± 7
Surface temperature (°C)	14.9 ± 0.2	17.1 ± 0.1
Surface salinity (psu)	33.51 ± 0.00	33.42 ± 0.01
Nitrate, mixed layer (μM)	2.21 ± 0.6	0.14 ± 0.03
Silicic acid, mixed layer (μM)	0.92 ± 0.50	0.72 ± 0.46
Dissolved iron, mixed layer (nM)	0.103 ± 0.007	0.098 ± 0.005
Chlorophyll *a* (mg Chl *a* m^{-2})	69 ± 10	22 ± 1
Autotroph carbon (mg C m^{-2})	1820 ± 310	780 ± 30
Heterotrophic protist carbon (mg C m^{-2})	380 ± 6	220 ± 40
Mesozooplankton: day (mg C m^{-2})	480 ± 180	440 ± 23
Mesozooplankton: night (mg C m^{-2})	1710 ± 2	860 ± 86
Migrating mesopelagics (mg WW m^{-2})	1400 ± 200	800 ± 400
^{14}C-primary production (mg C m^{-2} day^{-1})	1670 ± 308	325 ± 45
Phytoplankton growth rate (day^{-1})	0.80 ± 0.02	0.28 ± 0.05
Microzooolankton grazing rate (day^{-1})	0.18 ± 0.10	0.13 ± 0.04
Export: 60-m thorium (mg C m^{-2} day^{-1})	119	136
Export: 60-m traps (mg C m^{-2} day^{-1})	128 ± 27	112 ± 12

Chlorophyll and microplankton biomass are depth-integrated to 80 m, primary production and chlorophyll normalized mean rates of phytoplankton growth and microzooplankton grazing are to 50 m, mesozooplankton are from oblique 200-μm mesh bongo net samples to 210-m maximum depth, and migrating mesopelagic fish are based on day–night differences in multi-beam acoustical backscatter in the upper 200 m (Lara Lopez *et al.*, 2012).

Northern waters were notably higher in phytoplankton (autotroph carbon and Chl *a*) and in the portion of the zooplankton community undergoing nocturnal migration into the euphotic zone, i.e. the difference between nighttime and daytime biomass estimates. Higher plankton stocks in the northern waters were associated with higher nutrients, higher specific rates of phytoplankton growth and 5-fold higher rates of primary production. However, the higher standing stocks and production rates in the northern waters did not translate into substantially higher concurrent estimates of export production, determined both from the carbon collected directly in traps below the euphotic zone and calculated from the measured ^{234}Th deficiency in surface waters and the mean C:^{234}Th ratios in pump and trap samples (Stukel, 2011). The agreement between these two assessments is notable because they relate to different time scales of export flux (daily versus weekly to monthly integrated rates) and because sampling for the Th deficiency estimates were taken at the location of the experimental drift array. The sediment trap and incubation bottle arrays drifted closely together during Cycle 6, but diverged substantially during Cycle 5 with the trap

Downloaded from http://plankt.oxfordjournals.org/ at University of California, San Diego on October 19, 2012

array advecting quickly to the front, where it could have sampled particles produced under different conditions.

The repeated frontal crossings with the Moving Vessel Profiler illustrated that the front was a continuous feature with local enrichment of Chl *a* and LOPC-detected particles at each of the five crossings as the survey moved from west to east (Ohman *et al.*, 2012). At the resolution of the standard CTD-rosette transect sampling across the A-Front, the frontal transition was marked physically by a strong density gradient with the sigma 24.4 and 24.6 isopycnals outcropping at the front (Fig. 3A). Below the surface, the warmer southern waters overlaid a sharp pycnocline at ~40 m, under which signature low-salinity waters of the CC appeared as a layer between 40 and 60 m (Fig. 3B). Isopycnal surfaces shoaled sharply to the north across the section and particularly at the front (Stns 4 and 5), where low salinity CC waters extended into and mixed with the near-surface waters between the 24.6 and 24.8 sigma-θ surfaces (Fig. 3B). Notably, concentrations of dissolved nutrients (nitrate and silicic acid) showed modest enrichment between these density surfaces at the front relative to waters at comparable depths to the north and south (Fig. 3C and D). Larger effects are evident however in Chl *a* fluorescence and beam transmission, indicating substantial subsurface accumulations of phytoplankton and particles in the frontal zone (Fig. 3E and F).

SUMMARY OF MAJOR RESULTS

Expanding upon the brief overview of basic observations above, the accompanying papers in this issue provide a comprehensive assessment, from microbes to fish, of altered pelagic community biomass and composition across the A-Front transition. A plankton model, based on regional rate relationships and computationally derived estimates of nutrient fluxes across the front, provides further insights into plankton dynamics and biomass accumulation at the front (Li *et al.*, 2012). Lastly, the broader context of frontal impacts in the CC ecosystem is considered in a statistical analysis of spatial and temporal patterns of front occurrence in the region based on satellite imagery (Kahru *et al.*, 2012). The major findings of these companion studies are summarized below:

(i) Autotroph carbon was strongly elevated at the front, and large chain-forming diatoms uniquely dominated the subsurface biomass maximum. The front separated photosynthetic bacterial groups, with *Prochlorococcus* dominant in the south, *Synechococcus* dominant in the north and a local minimum of photosynthetic bacterial biomass at the front (Taylor *et al.*, 2012).

(ii) Strong linear relationships were found between chlorophyll fluorescence reading from ALF and total autotroph carbon biomass across the A-Front section, and between phycobiliprotein fluorescence and *Synechococcus* biomass in surface waters. Variable fluorescence (F_v/F_m), an indicator of phytoplankton photosynthetic efficiency, was elevated at the front. High-resolution underway sampling with ALF revealed a sharp peak in *Synechococcus* in a narrow zone of increasing temperature and surface salinity minimum at the front (Chekalyuk *et al.*, 2012).

(iii) Inherent and apparent optical properties showed strong gradients across the front. Enhanced beam attenuation, spectral diffuse attenuation and backscattering coefficients were consistent with higher concentrations and larger cell sizes just below the mixed layer at the front. Phytoplankton in this area had the highest quantum yield of photosynthesis and low values of both absorption and beam attenuation per unit of Chl *a*. In aggregate, the bio-optical patterns are consistent with large cells acclimated to low light and high nutrients at the front (Wang *et al.*, unpublished results).

(iv) Enhancements of the microbial habitat at the front were evident as local maxima in particulate and total organic nitrogen, bacterial carbon production, frequency of dividing cells and larger cell sizes (but not abundance) of bacteria. The ratio of viruses to bacteria was high at the front, while abundance of heterotrophic flagellates was depressed (Samo *et al.*, 2012).

(v) The front was a region of elevated abundance of suspension-feeding zooplankton, including calanoid copepods, copepod nauplii, *Oithona* spp., euphausiids and appendicularians. An index of secondary production, the ratio of nauplii copepod^{-1}, was elevated at the front. *In situ* imaging revealed that large organic aggregates were also several times more concentrated at the front than in adjacent waters (Ohman *et al.*, 2012).

(vi) The front marked a faunal boundary for vertically migrating mesopelagic fishes, euphausiids and larval fish, but not for non-migratory mesopelagic species. Bioacoustics indicated a dense surface aggregation of fish at the front and subsurface euphausiid aggregations beginning at the front and extending north (Lara Lopez *et al.*, 2012).

(vii) Thorpe-scale analysis of hydrographic data from the MVP indicates increased flux of nitrate into

Downloaded from http://plankt.oxfordjournals.org/ at University of California, San Diego on October 19, 2012

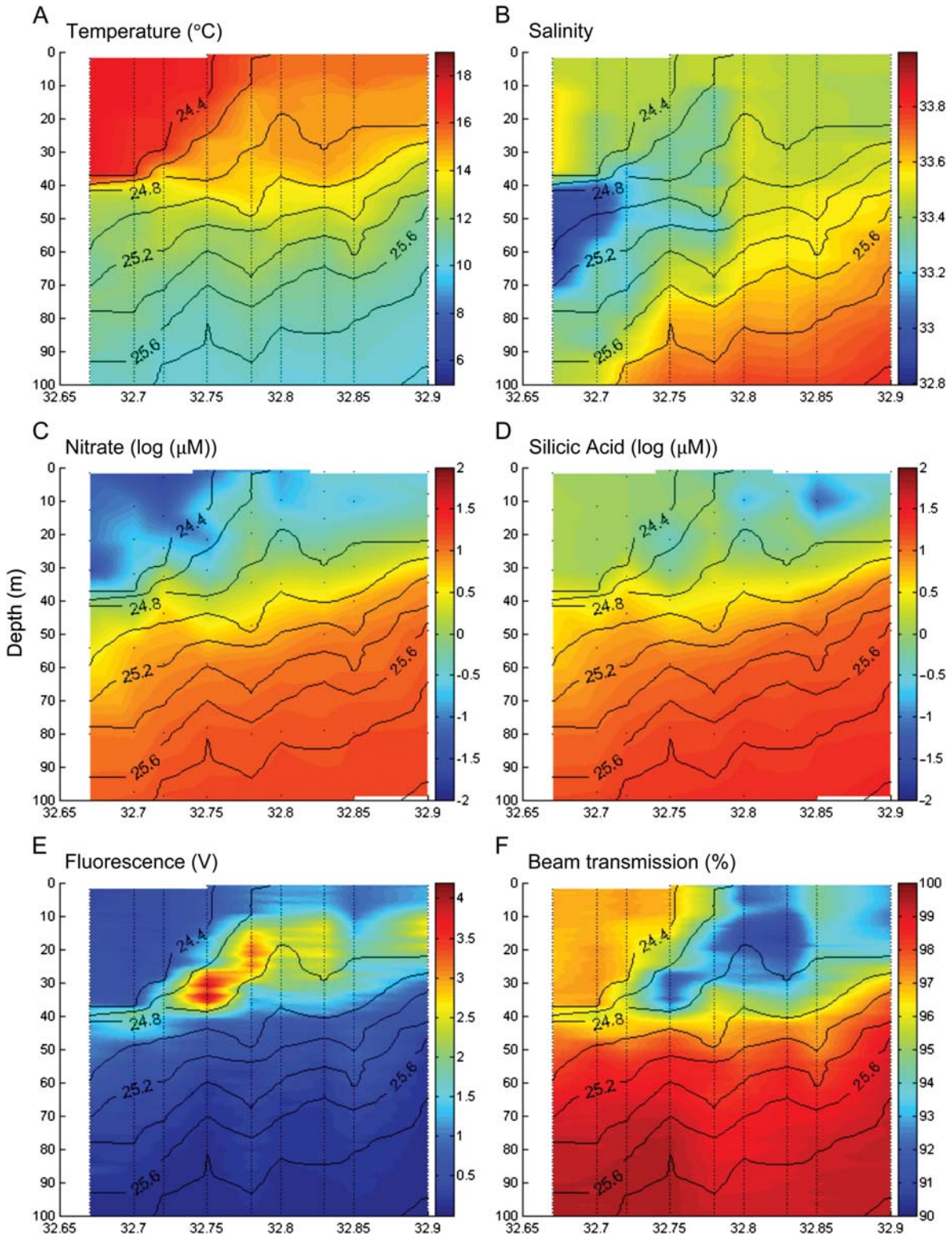

Fig. 3. Distribution of properties from CTD-rosette station sampling across the A-Front during the night of 24–25 October 2008. Cross-front sections are for (A) temperature, (B) salinity, (C) nitrate, (D) silicic acid, (E) chlorophyll fluorescence and (F) beam transmission. Isopycnal surfaces (sigma-t) are superimposed on each section. Locations of sampling stations are shown as dotted vertical lines.

Downloaded from http://plankt.oxfordjournals.org/ at University of California, San Diego on October 19, 2012

the euphotic zone at the front. Modeling results based on the A-Front field data suggest that increased diffusive diapycnal flux of nitrate and reduced microzooplankton grazing both contributed to enhanced production and conditions favorable to large diatoms at the front (Li *et al.*, 2012).

(viii) Statistical analyses of surface Chl *a* and temperature fronts demonstrated that they occur frequently in a wide band of the CCE, with a core maximum of Chl *a* frontal activity ~300 km off of central and southern California. Front frequencies show multi-decadal increasing trends for the offshore region off of southern California and northern Mexico, coincident with decreasing SST and increasing Chl *a* (Kahru *et al.*, 2012).

As a whole, these studies demonstrate substantial enrichment in plankton biomass, activity and physiological potential at the A-Front, which distinguish the frontal zone from adjacent waters. They also suggest that front frequency in the southern CC ecosystem may be linked to long-term climate impacts, contributing to the regional trend in increasing mean chlorophyll concentration.

BIOLOGICAL ENHANCEMENT MECHANISMS

Previous studies of fronts in the southern CC ecosystem, whether due to different feature selection or to coarse sampling resolution (e.g. CTD stations 20-km apart), have not been able to document biological characteristics at fronts that set them apart from adjoining waters (Haury *et al.*, 1993; Venrick, 2000). The A-Front study was thus designed principally to determine whether fronts in this region could be significant local sites of enhanced plankton biomass and activity. While we did not seek to distinguish specific mechanisms that could lead to such effects, at least some insights can be gained from previous investigations of front hydrography and physics in the region and from observations from the present study.

The most direct mechanism to produce biological enhancement at the interface of two water masses would be if local secondary circulation led to the convergence of flow fields and enhanced residence times (e.g. Franks, 1992). An additional mechanism could occur if each water mass contained a resource in excess that limited growth in the other. Surface waters advecting away from the Point Conception area, for example, often retain high excess nitrate concentrations because they are limited by the availability of the trace element iron (King and Barbeau, 2007, 2011). Therefore, elevated concentration of Fe in the low-nitrate southern waters could hypothetically provide the resource complement at the sites where the two waters mixed. Such a mechanism is readily dismissed by measurements of dissolved Fe during process Cycles 5 and 6, which show comparably low values for the upper mixed layer (Table I). In addition, if the answer were as simple as the mixing of two surface waters, one would expect to see prominent ribbons of enhanced Chl *a* in satellite images at frontal interfaces. To the contrary, the zone of strong phytoplankton response in A-Front was subsurface and invisible to satellites.

Based on vorticity calculations from the divergence velocities of drifter clusters, Chereskin and Niiler (Chereskin and Niiler, 1994) estimated the mean upwelling velocities of 5 m day^{-1} for the feature they studied during its eastward sweep across their study region. In the present study, estimates of diapycnal eddy diffusivity and nitrate fluxes were the highest in the area of the subsurface salinity minimum directly to the south of the frontal interface (Li *et al.*, 2012). Modeling suggests that this mechanism alone would have been sufficient to support biomass production similar to that observed at the A-Front, but simple isopycnal transport along the 24.6–24.8 density surfaces that uplifted at the front (Fig. 3) must also have contributed. There thus appears to be no shortage of explanations for how nutrients from below the euphotic zone could have arrived to support the subsurface phytoplankton bloom at the front. This does not address, however, how different substrates, nitrate, silicic acid and dissolved iron, related to one another as potentially limiting resources. All three of these elements are required by the large chain-forming diatoms that dominated in the frontal bloom, but particularly the latter two are needed in excess for diatoms to achieve a relative growth advantage over smaller, non-siliceous competitors (Landry *et al.*, 2008; Brzezinski *et al.*, 2011). The mean ratio of silicic acid to nitrate concentrations (2.4) in the salinity minimum water at 40–60 m south of the front exceeded the canonical 1:1 ratio thought to allow good growth of diatoms (Brzezinski, 1985). Waters with similar nitrate concentrations from 20 to 60 m depth north of the front had a relatively invariant silicic acid:nitrate ratio of 1.2. Mixing of the southern low salinity waters into the frontal area should therefore have provided the most favorable silica conditions for diatom growth.

Iron profile measurements were not made across the A-Front transect, but are available from waters adjacent to the front (Cycles 5 and 6) and from low salinity core waters of the CC directly west of the front study site (Cycle 2; http://cce.lternet.edu/data/cruises/cce-p0810/data/). All locations had comparable low estimates of mixed-layer Fe concentration (~0.1 nM;

Downloaded from http://plankt.oxfordjournals.org/ at University of California, San Diego on October 19, 2012

Table I), and comparable modest increases with depth below the euphotic zone. Four measurements made in low salinity (<33 psu) waters in the 50–100 m depth range give Fe concentrations of 0.19 ± 0.02 nM, which would imply a mean Fe:N ratio of 74 μmol mol N^{-1} for the salinity minimum waters that mixed into the front. Assuming Redfield C:N, that Fe:N ratio would support phytoplankton growth with a mean cell Fe:C cell quota of 11 μmol mol C^{-1}, which is approximately in the middle of values (6 versus ~20 μmol mol C^{-1}) measured for diatoms before and after a mesoscale iron enrichment experiment in the Southern Ocean (Twining *et al.*, 2004), and near the lower limit of values reported to support growth in a coastal diatom species (Sunda and Huntsman, 1995). The bioavailability of dissolved Fe in the present study is unclear, but the observed maximum in variable fluorescence ($F_v/F_m \approx 0.4$) in the area of diatom biomass accumulation at the front (Chekalyuk *et al.*, 2012) indicates that Fe must have arrived there in sufficient quantities to have stimulated photosynthetic potential. The less than optimal F_v/F_m readings are, however, consistent with the above nutrient ratio calculations in suggesting that the cells were likely still Fe deficient.

Given limited areal sampling along and around the A-Front, we do not have a coherent 3D perspective of flow fields and property distributions in the study area. It is therefore difficult to compare the physics and hydrography directly to previous investigations in the region or to assess the along-flow variability of system characteristics. The investigation could also have benefited from focused experimental studies along drifter paths in the area of maximal plankton concentrations at the frontal interface. Such measurements, planned for future studies, would help us to better understand the extent and variability of chemical and biological properties in frontal features, the relative roles of instantaneous local (e.g. imbalances in growth and grazing) versus upstream processes in producing and maintaining the unique front characteristics, and the downstream fates and export of production from the front versus adjacent waters.

ACKNOWLEDGEMENTS

We gratefully acknowledge the professionalism and numerous accommodations, large and small, of Captain Curl, the R/V *Melville* crew and resident technicians who greatly facilitated the sampling program. We also thank the many colleagues, students and technicians who contributed to the shipboard collections, post-cruise analyses and data presentations: A. Chekalyuk, P.J.S. Franks, J.A. Koslow, M. Picheral, K. Buck, Q. Li, B. Hopkinson, A. Lara Lopez, H. Wang, I. Ball, A. Cawood, P. Davison, M. Décima, A. Pasulka, B. Pedler, J. Powell, K. Roe, R. Rykaczewski, T. Samo, D. Taniguchi, A.G. Taylor, M. Hafez, D. Jenson, J. Liu, M. Roadman, J.-B. Romagnan, K. Semyanov, B. Seegers, D.A. Wick, J. Losh and M. Manzano-Sarabia.

FUNDING

The A-Front study was supported by U. S. National Science Foundation grants OCE 04-17616 and 10-26607 for the CCE LTER Program; and by the Gordon and Betty Moore Foundation (to M.D.O.).

REFERENCES

Basterretxea, G. and Aristegui, J. (2000) Mesoscale variability in phytoplankton biomass distribution and photosynthetic parameters in the Canary-NW African coastal transition zone. *Mar. Ecol. Prog. Ser.*, **197**, 27–40.

Brown, S. L., Landry, M. R., Selph, K. E. *et al.* (2008) Diatoms in the desert: phytoplankton community response to a mesoscale eddy in the subtropical North Pacific. *Deep-Sea Res. II*, **55**, 1321–1333.

Brzezinski, M. A. (1985) The Si:C ratio of marine diatoms. Interspecific variability and the effect of some environmental variables. *J. Phycol.*, **21**, 347–357.

Brzezinski, M. A., Baines, S., Balch, W. M. *et al.* (2011) Co-limitation of diatoms by iron and silicic acid in the equatorial Pacific. *Deep-Sea Res. II*, **58**, 493–511.

Centurioni, L. R., Ohlmann, J. C. and Niiler, P. P. (2008) Permanent meanders in the California Current System. *J. Phys. Oceanogr.*, **38**, 1690–1710.

Chekalyuk, A. and Hafez, M. (2008) Advanced laser fluorometry of natural aquatic environments. *Limnol. Oceanogr. Meth.*, **6**, 591–609.

Chekalyuk, A. M., Landry, M. R., Goericke, R. *et al.* (2012) Laser fluorescence analysis of phytoplankton across a frontal zone in the California Current ecosystem. *J. Plankon Res.*, **34**, 761–777.

Chereskin, T. K. and Niiler, P. P. (1994) Ciculation in the Ensenada Front—September 1988. *Deep-Sea Res.*, **41**, 1251–1287.

Fiala, M., Sournia, A., Claustre, H. *et al.* (1994) Gradients of phytoplankton abundance, composition and photosynthetic pigments across the Almeria-Oran front (SW Mediterranean Sea). *J. Mar. Syst.*, **5**, 223–233.

Franks, P. J. S. (1992) Phytoplankton blooms at fronts—patterns, scales and forcing mechanisms. *Rev. Aquat. Sci.*, **6**, 121–137.

Gorsky, G., Ohman, M. D., Picheral, M. *et al.* (2010) Digital zooplankton image analysis using the zooscan integrated system. *J. Plankton Res.*, **32**, 285–303.

Haury, L. R., Venrick, E. L., Fey, C. L. *et al.* (1993) The Ensenada Front: July 1985. *CalCOFI Reports*, **34**, 69–88.

Herman, A. W., Beanlands, B. and Phillips, E. F. (2004) The next generation of optical plankton counter: the laser-OPC. *J. Plankton Res.*, **26**, 1135–1145.

Downloaded from http://plankt.oxfordjournals.org/ at University of California, San Diego on October 19, 2012

Hickey, B. M. (1998) Coastal oceanography of western North America from the tip of Baja California to Vancouver Island. In Robinson, A. R. and Brink, K. H. (eds), *Coastal Segment, The Sea*. J. Wiley and Sons, Inc., New York, pp. 345–391.

Hill, A. E., Hickey, B. M., Shillington, F. A. *et al.* (1998) Eastern boundary currents: a pan-regional review. In Robinson, A. R. and Brink, K. H. (eds), *The Sea*. J. Wiley and Sons Inc., New York, pp. 29–67.

Hood, R. R., Abbott, M. R. and Huyer, A. (1991) Phytoplankton and photosynthetic light response in the coastal transition zone off northern California in June 1987. *J. Geophys. Res.*, **96**, 14769–14780.

Jacquet, S., Prieur, L., Avois-Jacquet, C. *et al.* (2002) Short-timescale variability of picophytoplankton abundance and cellular parameters in surface waters of the Alboran Sea (western Mediterranean). *J. Plankton Res.*, **24**, 635–651.

Kahru, M., Di Lorenzo, E., Manzano-Sarabia, M. *et al.* (2012) Spatial and temporal statistics of sea surface temperature and chlorophyll fronts in the California Current. *J. Plankton Res.*, **34**, 749–760.

King, A. L. and Barbeau, K. (2007) Evidence for phytoplankton iron limitation in the southern California System. *Mar. Ecol. Prog. Ser.*, **342**, 91–103.

King, A. L. and Barbeau, K. A. (2011) Dissolved iron and macronutrient distributions in the southern California Current System. *J. Geophys. Res.*, **116**, C03018, doi:10.1029/2010JC006324.

Knauer, G. A., Martin, J. H. and Bruland, K. W. (1979) Fluxes of particulate carbon, nitrogen, and phosphorus in the upper water column of the Northeast Pacific. *Deep-Sea Res.*, **26**, 97–108.

Landry, M. R., Brown, S. L., Rii, Y. M. *et al.* (2008) Depth-stratified phytoplankton dynamics in Cyclone *Opal*, a subtropical mesoscale eddy. *Deep-Sea Res. II*, **55**, 1348–1359.

Landry, M. R., Ohman, M. D., Goericke, R. *et al.* (2009) Lagrangian studies of phytoplankton growth and grazing relationships in a coastal upwelling ecosystem off Southern California. *Prog. Oceanogr.*, **83**, 208–216.

Lara Lopez, A. L., Davison, P. and Koslow, J. A. (2012) Abundance and community composition of micronekton across a front off Southern California. *J. Plankton Res.*, **34**, 828–848.

Li, Q. P., Franks, P. J. S., Ohman, M. D. *et al.* (2012) Enhanced nitrate fluxes and biological processes at a frontal zone in the southern California Current system. *J. Plankton Res.*, **34**, 790–801.

Loggerwell, L. A., Lavaniegos, B. and Smith, P. E. (2001) Spatially-explicit bioenergetics of Pacific sardine in the Southern California Bight: are mesoscale eddies areas of exceptional prerecruit production. *Prog. Oceanogr.*, **49**, 391–406.

Lynn, R. J. and Simpson, J. J. (1987) The California Current system: the seasonal variability of its physical characteristics. *J. Geophys. Res.*, **92**, 12947–12966.

Marchesiello, P., McWilliams, J. C. and Shchepetkin, A. (2003) Equilibrium structure and dynamics of the California Current system. *J. Phys. Oceanogr.*, **33**, 753–783.

Niiler, P. P., Poulain, P. M. and Haury, L. R. (1989) Synoptic 3-dimensional circulation in an offshore-flowing filament of the California Current. *Deep-Sea Res.*, **36**, 385–405.

Niiler, P. P., Sybrandy, A. S., Bi, K. N. *et al.* (1995) Measurements of the water-following capability of holey-sock and tristar drifters. *Deep-Sea Res.*, **42**, 1951–1964.

Ohman, M. D., Powell, J., Picheral, M. *et al.* (2012) Mesozooplankton and particulate matter responses to a deep-water frontal system in the southern California Current System. *J. Plankton Res.*, **34**, 815–827.

Ohman, M. D. and Wilkinson, J. R. (1989) Comparative standing stocks of mesozooplankton and macrozooplankton in the southern sector of the California Current system. *Fish. Bull.*, **87**, 967–976.

Pares-Sierra, A. and O'Brien, J. J. (1989) The seasonal and interannual variability of the California Current system: a numerical model. *J. Geophys. Res.*, **94**, 3159–3180.

Picheral, M., Guidi, L., Stemmann, L. *et al.* (2010) The underwater vision profiler 5: an advanced instrument for high spatial resolution studies of particle size spectra and zooplankton. *Limnol. Oceanogr. Meth.*, **8**, 462–473.

Pitcher, G. C., Boyd, A. J., Horstman, D. A. *et al.* (1998) Subsurface dinoflagellate populations, frontal blooms and the formation of red tide in the southern Benguela upwelling system. *Mar. Ecol. Prog. Ser.*, **172**, 253–264.

Rykaczewski, R. R. and Checkley, D. M. (2008) Influence of ocean winds on the pelagic ecosystem in upwelling regions. *Proc. Natl Acad. Sci. USA*, **105**, 1065–1970.

Samo, T. J., Pedler, B. E., Ball, I. G. *et al.* (2012) Microbial distribution and activity across a water mass frontal zone in the California Current Ecosystem. *J. Plankton Res.*, **34**, 802–814.

Strub, P. T., Kosro, P. M., Huyer, A. *et al.* (1991) The nature of the cold filaments in the California Current System. *J. Geophys. Res.*, **96**, 14743–14768.

Stukel, M. R. (2011) Biological control of vertical carbon flux in the California Current and equatorial Pacific. Ph.D. dissertation. University of California, San Diego, 229 pp.

Stukel, M. R., Landry, M. R., Benitez-Nelson, C. R. *et al.* (2011) Trophic cycling and carbon export relationships in the California Current ecosystem. *Limnol. Oceanogr.*, **56**, 1866–1878.

Sunda, W. G. and Huntsman, S. A. (1995) Iron uptake and growth limitation in oceanic and coastal phytoplankton. *Mar. Chem.*, **50**, 189–206.

Taylor, A. G., Goericke, R., Landry, M. R. *et al.* (2012) Sharp gradients in phytoplankton community structure across a frontal zone in the California Current Ecosystem. *J. Plankton Res.*, **34**, 778–789.

Twining, B. S., Baines, S. B., Fisher, N. S. *et al.* (2004) Cellular iron contents of plankton during the Southern Ocean Iron Experiment (SOFeX). *Deep-Sea Res. I.*, **51**, 1827–1850.

Venrick, E. L. (2000) Summer in the Ensenada Front: the distribution of phytoplankton species, July 1985 and September 1988. *J. Plankton Res.*, **22**, 813–841.

Wang, H., Mitchell, B. G., Chekalyuk, A. *et al.* (2008) Influence of phytoplankton community structure on photosynthetic physiology and bio-optics in southern California Current Ecosystem. 2008 Ocean Science Meeting, 2–7 March 2008, Orlando, FL.

Downloaded from http://plankt.oxfordjournals.org/ at University of California, San Diego on October 19, 2012